

## Accepted Manuscript

Title:  $\text{CrO}_x/\text{SiO}_2$  catalysts prepared by metal vapour synthesis: physical-chemical characterisation and functional testing in oxidative dehydrogenation of propane

Authors: M.A. Botavina, C. Evangelisti, Yu.A. Agafonov, N.A. Gaidai, N. Panziera, A.L. Lapidus, G. Martra



PII: S1385-8947(10)01166-6  
DOI: doi:10.1016/j.cej.2010.11.070  
Reference: CEJ 7519

To appear in: *Chemical Engineering Journal*

Received date: 13-4-2010  
Revised date: 8-11-2010  
Accepted date: 19-11-2010

Please cite this article as: M.A. Botavina, C. Evangelisti, Yu.A. Agafonov, N.A. Gaidai, N. Panziera, A.L. Lapidus, G. Martra,  $\text{CrO}_x/\text{SiO}_2$  catalysts prepared by metal vapour synthesis: physical-chemical characterisation and functional testing in oxidative dehydrogenation of propane, *Chemical Engineering Journal* (2010), doi:10.1016/j.cej.2010.11.070

This is a PDF file of an unedited manuscript that has been accepted for publication. As a service to our customers we are providing this early version of the manuscript. The manuscript will undergo copyediting, typesetting, and review of the resulting proof before it is published in its final form. Please note that during the production process errors may be discovered which could affect the content, and all legal disclaimers that apply to the journal pertain.

**CrO<sub>x</sub>/SiO<sub>2</sub> catalysts prepared by metal vapour synthesis: physical-chemical characterisation  
and functional testing in oxidative dehydrogenation of propane**

M.A. Botavina<sup>a,b\*</sup>, C. Evangelisti<sup>c</sup>, Yu.A. Agafonov<sup>b</sup>, N.A. Gaidai<sup>b</sup>, N. Panziera<sup>c</sup>, A.L. Lapidus<sup>b</sup>, G.  
Martra<sup>a,d</sup>.

<sup>a</sup> Department of Chemistry IFM and NIS Centre of Excellence, University of Torino, via P.Giuria,  
7, 10125, Torino, Italy, <sup>b</sup> N.D.Zelinsky Institute of Organic Chemistry, Russ.Acad.Sci., Moscow,  
Russia, <sup>c</sup> Department of Chemistry and Industrial Chemistry and Advanced Catalysts S.r.l.,  
University of Pisa, via Risorgimento 35, 56126 Pisa, Italy, <sup>d</sup> associated to ISTM-CNR, Via C. Golgi,  
19, 20133 Milan, Italy

\*Corresponding author: phone: +39 - 011 6707507, FAX: +39 - 011 6707855, e-mail:  
maria.botavina@unito.it

**Abstract**

In the present work catalysts prepared by a new perspective method of metal vapour synthesis were studied in the reaction of propane oxidative dehydrogenation in the presence of CO<sub>2</sub> as a mild oxidant. This method let to obtain on the catalyst surface a high dispersed chromium species even at high chromium loadings. On the surface of the catalysts with the chromium loading up to 6.0 wt % only chromate species were found, the further increase of the chromium loading results in the appearance of the  $\alpha$ -Cr<sub>2</sub>O<sub>3</sub>. The catalyst with 6.0 wt % demonstrated also the highest catalytic activity with the yield in propene 69%.

**Keywords:** Cr/SiO<sub>2</sub>, Metal Vapour Synthesis, DR UV-Vis spectroscopy, IR spectroscopy of adsorbed NH<sub>3</sub>, propane oxidative dehydrogenation; CO<sub>2</sub>.

## 1. Introduction

Supported chromium catalysts play a relevant role in many important industrial chemical processes, both actual (e.g, the Phyllips catalysts of the polymerization of ethene [1-4]) and perspective. Among these latter is the oxidative dehydrogenation of propane (ODH), where O<sub>2</sub>, CO<sub>2</sub> or a CO<sub>2</sub>+O<sub>2</sub> mixture can be used like an oxidant agents [5-14]. Actually, this process has been the subject of many investigations, and a number of catalysts has been evaluated [15]. However, catalysts based on Cr are among the more effective, and the optimisation of their behaviour is still a target to be attained. In this respect, a basic point is represented by the achievement of a high dispersion of chromium, as isolated/oligomeric CrO<sub>x</sub> species are supposed to exhibit the highest catalytic activity. The traditional preparation method based on wet impregnation is characterized by a low cost and operational easy, but it appeared unable to prevent the formation of agglomerated species and Cr<sub>2</sub>O<sub>3</sub> particles, that are less effective or even effective towards side reactions (e.g, total oxidation) respectively. Conversely, "one-pot" methods for the preparation of Cr/MCM-41 [9, 10, 16] and Cr/SBA-15 [17, 18] materials with highly isolated Cr species exposed at the inner wall of the channels of a silica regular mesoporous matrix have been developed, but Cr contents higher than 1 wt% usually resulted in the depletion of the mesoporous structure. Here, we report the possibility to prepare Cr/SiO<sub>2</sub> catalysts for ODH by using the so called "metal vapour synthesis (MVS) method". The co-condensation at low temperature of metal vapour (commonly produced on lab scale by resistance heating and on larger scale by electron beam vaporization) with vapour of weakly stabilizing organic ligands (such as mesitylene, acetone or acetonitrile), using commercially available reactors [19], affords solvent-stabilized metal atoms (Solvated Metal Atoms, SMA) soluble in the excess of ligand [20,21]. Depending from the kind of the organic ligand SMA can affords well defined organo-metallic species [22] or solvent stabilized metal clusters suitable for the preparation of supported metal systems on a wide range of organic and inorganic materials[23-26]. Thus, this method appear as a good candidate for the attainment of a high dispersion of supported species even at quite high loading. Actually, the presence of a high

amount of possibly isolated Cr species is among the basic requirement for setting up highly active ODH catalysts, that, if characterized also by a good selectivity and stability, could be of interest for actual applications. In this paper we report on  $\text{CrO}_x/\text{SiO}_2$  catalysts prepared by metal vapour synthesis that were tested in the reaction of propane oxidative dehydrogenation using a mild oxidant ( $\text{CO}_2$ ).

## 2. Material and methods

Catalysts (here/after Cr-SiO<sub>2</sub>-MVS) were prepared using metal vapour synthesis (MVS) [19-26]. According to that method chromium (800 mg) was sublimed by resistive heating in a alumina coated tungsten wire crucible. Chromium vapour were co-condensed with mesitylene vapour (60 mL) on the cooled walls of a previously described glass reactor [21] maintained at the liquid nitrogen temperature (-196°C) for 1 hour. As a result it was obtained a solid matrix which, at the end of the reaction, was allowed to melt under vacuum at ca. -40°C simply removing the nitrogen liquid bath and warming up the solution at 25°C. The resulting deep red solution containing mono- and oligonuclear chromium-mesitylene species [22] was worked up under dry argon atmosphere with the use of standard Schlenk techniques and kept at 25°C. The amount of chromium in the above solutions was evaluated by Inductively Coupled Plasma-Optical Emission Spectrometers (ICP-OES) with a Spectro-Genesis instrument, using a software Smart Analyzer Vision. The support (commercial silica KSKG, Russia) was ground and sieved to obtain the fraction with particle size in the 0.25 - 0.5 mm and than this fraction was calcined in air flow at 600°C for 2 hours.

The deep red [Cr-mesitylene] solution was added to an appropriate amount of a suspension of the support in mesitylene under dry argon atmosphere and was stirred at room temperature until the liquid phase became colorless (overnight). The organic phase was than removed via syringe and powdered catalyst was washed with *n*-pentane and dried under vacuum at room temperature, than calcined at 600°C in air flow for 2 hours.

Catalytic studies were carried out in a flow-reactor at  $T = 600^{\circ}\text{C}$  and atmospheric pressure. The composition of the reaction feed was:  $\text{C}_3\text{H}_8 : \text{CO}_2 : \text{N}_2 = 15 : 30 : 55$ . Before the reaction all catalysts were activated in air flow at  $T=600^{\circ}\text{C}$  for at least 2 hours. The reaction products were analysed by GC methods using two columns – molecular sieves 5A ( $\text{H}_2$ ,  $\text{O}_2$ ,  $\text{N}_2$ ,  $\text{CH}_4$ ,  $\text{CO}$ ) and Porapak Q ( $\text{CO}_2$ , hydrocarbons). After the experiment catalysts were regenerated in air flow at  $T=600^{\circ}\text{C}$  for 6 hours.

Specific surface areas (SSA) were measured with a Micromeritics ASAP 2010 by nitrogen adsorption at 77 K following the BET model, while pore volume and size were calculated by using the BJH model (adsorption branch). Before measurements all samples were outgassed at  $200^{\circ}\text{C}$  until a residual pressure  $1.0 \times 10^{-4}$  Torr (1 Torr: 133.33 Pa).

Observations and analysis of the powders by transmission electron microscopy coupled with energy dispersive X-ray spectroscopy (TEM-EDS) were performed with a JEOL 3010-UHR instrument (acceleration potential of 300 kV) equipped with an Oxford Inca Energy TEM 200 EDS X-rays analyzer. To obtain a good dispersion and avoid any contamination, lacey carbon Cu grids were briefly contacted with the powders, resulting in the adhesion of some particles to the sample holders by electrostatic interactions. When EDS was used in mapping mode, the Cr  $K\alpha$  emission at 5.4 kV was selected.

Diffuse Reflectance UV-Vis spectroscopy (DR UV-vis) measurements were performed with a Perkin-Elmer Lambda19 instrument equipped with an integrating sphere with the internal surface covered inside with  $\text{BaSO}_4$ . The catalysts (diluted with bare silica in a 1 : 12 rates by weight) were placed in a flow reactor connected with a side branch sealed with an optical quartz cell for the UV-Vis measurements. The samples were treated in the reactor at  $600^{\circ}\text{C}$  under flow of oxygen for 2h, than cooled to room temperature and kept in static  $\text{O}_2$ . The powder was then transferred in the side branch for the UV-Vis measurements.

FTIR spectra were collected using Vector 22 spectrometer equipped with a MCT detector and running at  $4 \text{ cm}^{-1}$  resolution. The catalyst powders were pressed in self supported pellets and

placed in a quartz cell with KBr windows that allow all necessary thermal treatments and the subsequent adsorption of the probe molecule ( $\text{NH}_3$ ) without exposure the catalyst pellet to air. Before IR measurements the samples were heated in 100 Torr of  $\text{O}_2$ ,  $T=550^\circ\text{C}$ , 1h and than outgassed at the same temperature for 1h (residual pressure  $1,0\times 10^{-5}$  Torr, 1 Torr : 133.33 Pa). Spectra of absorbed  $\text{NH}_3$  are reported in Absorbance after subtraction of the IR pattern before  $\text{NH}_3$  admission onto the sample. High purity  $\text{NH}_3$  (Matheson) was used dried by passing through a trap cooled with solid/liquid ethanol mixture before admission in the cell.

### 3. Results and discussion

#### Textural features of the catalysts

Catalysts Cr-SiO<sub>2</sub>-MVS with Cr loading from 0.25 to 6.0 wt% exhibited a specific surface area ca. 310 m<sup>2</sup>/g with a slight decrease of the total pore volume with an increase of the chromium content (Table 1, Part A). The catalyst with Cr loading of 10.0 wt% showed a decrease of specific surface area of ca. 20% with a further loss of total pore volume and a sharp decrease of average pore diameter that should result from the filling or blockage of the smallest pores by chromium species.

---

*Please, insert here Table 1*

---

For the sake of comparison, the values for the catalysts prepared by wet impregnation method (hereafter: Cr-SiO<sub>2</sub>-WI) are also reported [5] (Table 1, Part B). It can be observed, that the two types of catalysts with the similar chromium loadings exhibit similar textural features.

The pore size distribution remained monomodal (the highest pore fraction with the size 14 nm) for all studied samples. Up to the Cr loading of 6.0 wt% the porosity of the catalysts was similar to that exhibited by the bare support, indicating that highly dispersed chromium particles do

not block silica pores. Conversely, the increase of Cr loading up to 10.0 wt% resulted in the decrease of the pore size that can be due to the formation of bulky supported species on the silica surface.

Such an evolution of textural features was accounted by changes in structure and morphology observed by TEM. The samples with Cr loading up to 6.0 wt% appeared constituted by irregular particles, mainly constituted by SiO<sub>2</sub>, as checked by EDS (Fig. 1A). In addition a mapping of the location of Cr and Si was carried out by EDS, and the contours of the obtained maps appeared almost coincident with the borders of the particles aggregates, observed in the corresponding TEM images, suggesting the presence of highly dispersed Cr on the silica surface (Fig. 1B and C).

---

*Please, insert here Figure 1*

---

At Cr 10 wt% loading also big prismatic particles were clearly observed (Fig. 2A). EDS revealed that they are essentially composed by Cr and O (Fig. 2B), and on the basis of the spectroscopic data reported in the following, they can be identified as  $\alpha$ -Cr<sub>2</sub>O<sub>3</sub> particles. In the bigger fragment of the catalyst the presence of Si is also observed (Fig. 2C).

---

*Please, insert here Figure 2*

---

#### DR UV-Vis spectroscopy

All samples were re-calcined in the UV-Vis cell in flowing O<sub>2</sub> and DR UV-Vis spectra of the not re-exposed to air catalysts were recorded (Figure 3, panel A). For the sake of comparison, the spectra of the catalysts, prepared by wet impregnation (Figure 3, panel B) and the spectrum of the bare silica KSKG (Figure 3, panel B, curve 1) are also reported [5].



---

*Please, insert here Figure 3*

---

Bands at ca. 40000, 27000 (with an ill resolved shoulder at ca. 30000  $\text{cm}^{-1}$ ), and 21500  $\text{cm}^{-1}$  are present in the spectra of all catalysts, prepared by both methods. The presence of these bands is the evidence of oxygen to  $\text{Cr}^{6+}$  CT transitions of monochromates, di- and/or polychromates grafted to the  $\text{SiO}_2$  surface [27a, 28]. The bands at 40000 and 21500  $\text{cm}^{-1}$  did not appear structured enough to distinguish the contribution of each of these species, while the sub-bands at ca. 30000  $\text{cm}^{-1}$  and 27000  $\text{cm}^{-1}$  can be attributed to di-and/or polychromates and monochromates, respectively. By increasing the Cr loading from 0.25 to 6.0 wt% (Figure 3, panel A, curves 1-5) all mentioned bands progressively increased in intensity and underwent a light shift towards high frequency, but no other band was observed. At a higher Cr loading 10.0 wt% the intensity of the bands at 40000, 27000 and 21500  $\text{cm}^{-1}$  increased insignificantly and a new band at 16500  $\text{cm}^{-1}$  that can be assigned to the lowest CT transition occurring in  $\alpha\text{-Cr}_2\text{O}_3$  was observed, while in the spectra of Cr- $\text{SiO}_2$ -WI catalysts this band (16500  $\text{cm}^{-1}$ ) appeared at the chromium loading of 3.0 wt% already (Figure 3, panel B, curves 4-6). As the spectral changes occurred in such a region could be accounted by the presence of progressively increasing amount of di-and polychromates [39, a-c], it can be supposed that depositing chromium via metal vapour synthesis resulted in a higher dispersion of the supported phase. Such a results of DR UV-Vis measurements are in good correspondence with TEM-EDS data reported above.

#### FTIR spectroscopy of adsorbed $\text{NH}_3$

The presence of the Brønsted acid sites on the catalyst surface are an object of interest as such centres can promote the transformation of initially produced olefins, in particular starting the processes leading to the deactivation of the catalysts by cocking [29]. The catalysts were tested by adsorption of ammonia, monitored via IR. For the sake of simplicity, only the spectral range where bands due to the deformation modes of adsorbed  $\text{NH}_3$  and  $\text{NH}_4^+$  species will be presented, being

enough informative with respect to the scope of this work. The catalysts were pre-outgassed at high temperature, contacted with 20 Torr  $\text{NH}_3$  and then progressively outgassed until prolonged pumping at room temperature. IR spectra (not reported) indicated that at the end of this process ammonia molecules were completely desorbed from silanols, while components due to  $\text{NH}_3$  molecules adsorbed on  $\text{Cr}^{n+}$  sites, acting as Lewis acid centres, ammonium ions produced by interactions with Brønsted acid centres, if any, and other species resulting from chemical reactions between ammonia and surface sites underwent changes due to the removal of physisorbed ammonia solvating them only, while their desorption, in the adopted conditions, essentially did not occur. For this reason, only the spectra related to such irreversibly adsorbed species are shown in Figure 5. The data are normalized to both the mass and  $\text{SSA}_{\text{BET}}$  of the various materials, and then the intensity of the IR bands is proportional to the amount of the correspondent species per unit of surface area.

For the sake of comparison,  $\text{NH}_3$  adsorption was carried out on the bare  $\text{SiO}_2$  support, resulting in the spectrum in curve 1 (Figure 4, panel A), exhibiting only a very weak component at ca.  $1460\text{ cm}^{-1}$ , likely corresponding to the asymmetric deformation mode of ammonium ions formed on impurity traces having a Brønsted acid character. For the reference the same spectra on the catalysts, prepared by wet impregnation method, are reported in the Figure 4, panel B.

-----  
*Please, insert here Figure 4*  
 -----

As for the spectra obtained for the MVS catalysts containing the increasing amount of chromium (Figure 4, panel A, curves 2-6), in all cases they appeared dominated by band at  $1615\text{ cm}^{-1}$  due to the  $\delta_{\text{asym}}$  mode of ammonia molecules adsorbed on  $\text{Cr}^{n+}$  surface centres [30, 31]. Unfortunately, such a vibrational modes is poorly sensitive to the oxidation states (2+, 3+ or 6+) of the adsorbing chromium centres [30, 31], that, vice versa, could be probed by the features of the  $\delta_{\text{sym}}$  absorption, but it falls in the  $1300\text{-}1100\text{ cm}^{-1}$  range, then below the low frequency cut-off due to the silica support.

Moving towards lower frequency, the weak band at  $1555\text{ cm}^{-1}$ , can be attributed to the  $\delta\text{NH}_2$  mode of  $\text{Si-NH}_2$  species formed by reaction of  $\text{NH}_3$  with strained  $\text{Si-O-Si}$  (and/or  $\text{Si-O-Cr}$ ) bridges [32, 33]. The other product of this reaction should be  $\text{Si-OH}$  (and/or  $\text{Cr-OH}$ ) species, likely contributing to the broad and complex band in the  $\nu_{\text{OH}}$  region (not shown).

Finally, a broad absorption with maximum at ca.  $1445\text{ cm}^{-1}$  is present, due to asymmetric bending modes of adsorbed ammonium ions [30, 31]. The symmetric bending mode of such species is responsible for the very weak feature at ca.  $1680\text{ cm}^{-1}$ , so feeble because related to forbidden IR transitions [30].

As for the behavior of these spectral components in dependence on the Cr loading, it can be observed that the integrated intensity of both the signals related to adsorbed ammonia molecules and ammonium ions markedly did not change significantly for the samples with low Cr loadings (0.5 and 1.3 wt%) and then increase progressively with the increase of the chromium content (Figure 4, panel A, curves 2-6), whilst the integrated intensity of weaker band due to  $\text{Si-NH}_2$  species increased up to 2.5 wt% of chromium and that remains stable.

The heterogeneity of Cr species in the various catalysts evidenced by DR UV-Vis spectroscopy and the lack of sensitivity towards adsorbing centers of the band related to ammonia stabilized on such centers prevented the possibility to obtain specific information on Cr surface sites along the series of catalysts from the band at  $1615\text{ cm}^{-1}$ . However, the observed dependence of the integrated intensity of such band on the Cr loading indicates some possibility of the further increase of the amount of exposed Cr centres by increasing the Cr amount over 10.0 wt%, in agreement with the indication on the speciation and dispersion of Cr species obtained from DR UV-Vis data.

Passing to the components related to adsorbed ammonium ions, their presence clearly indicates that the supporting of chromium resulted also in the appearance of Brønsted acid sites. The dependence of the integrated intensity of the band at  $1445\text{ cm}^{-1}$  on the Cr loading, similar to that exhibited by the  $1615\text{ cm}^{-1}$  band, suggests that these acid centres could be related to “not three-dimensional” supported chromium species. Such a feature is similar to that reported in the literature

for  $V^{5+}$  [34-36] and  $Ti^{4+}$  [32]. The presence of Brønsted acid sites is of interest in the elucidation of the surface properties of the investigated catalysts, because, as reported in the literature devoted to paraffin dehydrogenation processes [29] these centres can promote the further transformation of initially produced olefins, in particular starting the processes leading to the deactivation of the catalysts by coking.

Finally, also the features related to the band at  $1555\text{ cm}^{-1}$  due to Si-NH<sub>2</sub> species resulting from reaction of ammonia with of Si-O-Si and/or Cr-O-Si strained bridges, deserve some comment. The appearance of this component, and then the related surface sites, resulted from the presence of chromium on the support. Strained Si-O-Si bridges, reactive toward ammonia, are known to be formed also on bare silica, but after outgassing treatment at significantly higher temperatures [37-39]. The formation of such particular structure is then apparently promoted by the involvement of the silica support in the fixation of chromium species. A similar behaviour was found in the case of  $Ti^{4+}$  centres dispersed on MCM-41 silica [32], although in that case the transition metal ions were introduced in the silica carrier through a one-pot synthesis. The other noticeable point is that the amount Si-NH<sub>2</sub> species, and then of parent Si-O-Si and/or Cr-O-Si strained bridges, increased up to the 2.5 wt% of the chromium loading, suggesting that the formation of such strained bridges is related to the formation of highly dispersed chromium species.

As for the behavior of the same components in the spectra of the catalysts, obtained by WI method, it can be observed that the integrated intensity of both the signals related to adsorbed ammonia molecules and ammonium ions markedly increase until the content of chromium is raised up to 3.0 wt%, and then increase less significantly (Figure 4, panel B), whilst the weaker band due to Si-NH<sub>2</sub> species exhibit essentially the same intensity independently of the Cr loading. The observed dependence on the integrated intensity of the band  $1615\text{ cm}^{-1}$  on the Cr loading indicates the decline of the possibility to further increase the amount of exposed Cr centres by increasing the Cr amount over 3.0 wt% for WI catalysts. At the same time the amount Si-NH<sub>2</sub> species, and then of parent Si-O-Si and/or Cr-O-Si strained bridges, did not depend on the Cr loading, suggested that the

highly dispersed chromium species was formed in essentially the same amount as the amount of supported Cr on the surface of WI catalysts was higher than 0.5 wt%.

The higher possibility of the increase of the amount of exposed Cr centres with the increase of Cr loading together with the observed increase of the formed Si–NH<sub>2</sub> species up to 2.5 wt% of chromium, monitors that by using the MVS method the higher dispersion of chromium species can be attained.

#### Catalytic tests

The initial propane conversion (x), selectivity toward olefins (S) and olefins yield (Y) for the catalysts with the different chromium loading prepared by MVS technique in the oxidative dehydrogenation of propane in the presence of CO<sub>2</sub> are reported in the Table 2.

-----  
*Please, insert here Table 2*  
-----

Catalyst that contains only 0.5wt% Cr already demonstrated propane conversion of ca.45% that is almost equal to the propane conversion that can be achieved on the catalyst with 5.0 wt% Cr but prepared by standard method of wet impregnation (47%) [5]. Propane conversion increased with the increase of chromium loading and on the catalyst with 6.0wt% of chromium attained 85%. The further increase of the chromium loading up to 10.0 wt% do not result in the additional increase of propane conversion – it remains on the level of 80%. Taking into account that the specific surface area of the catalyst with 10.0 wt% Cr is ca. 20% lower than that of the catalyst with 6.0 wt% Cr the catalyst with the higher chromium loading (10.0 wt%) exhibited even superior hydrocarbon conversion per unit of surface area. As concerns propene selectivity its values slightly decrease with an increase of the chromium content (from 87% at 0.25 wt% Cr to 78 at 10.0 wt% Cr). Selectivity to ethylene was on the level of 7-8% in all investigated range of the chromium loading. On catalyst with chromium loading of 6.0wt% total olefin yield reach 68%.

The results of the long-term tests for the MVS catalyst with 0.5 wt% chromium loading are reported in Figure 5, curves “1”. For the sake of comparison on the same Figure the results of the similar test for the WI catalyst with ten time higher chromium loading (5.0 wt%) are presented (curves “2”) [5].

---

*Please, insert here Figure 5*

---

The initial conversion of propane on the 0.5-Cr/SiO<sub>2</sub>-MVS catalyst was ca. 42%, than in 400 minutes decreased till ca. 28% and then remained stable for the next 400 minutes (Figure 6, Panel A). In the same reaction conditions the initial conversion of propane on the 5.0-Cr/SiO<sub>2</sub>-WI catalyst reached ca. 45% and than in 400 minutes reduced till ca. 30% and continue to decrease.

As for total olefin selectivity (Figure 5, Panel B, curves a) for the both catalysts the close results were obtained (ca. 94% for 5.0-Cr/SiO<sub>2</sub>-WI catalyst and ca. 92.5% for 0.5-Cr/SiO<sub>2</sub>-MVS catalyst). Since the propane conversions and total olefin selectivity were almost the same the total olefin yields appeared also similar (Figure 5, Panel B, curves b). For the 0.5-Cr/SiO<sub>2</sub>-MVS catalyst it was ca. 40% in the beginning and than decrease till ca. 25%, and for 5.0%Cr/SiO<sub>2</sub>-WI catalyst it falls down from initially 41% till ca. 30%.

Almost equal catalytic activity of 0.5-Cr/SiO<sub>2</sub>-MVS and 5.0%Cr/SiO<sub>2</sub>-WI catalysts supposed that due to the higher dispersion of chromium species the amount of active centers on the surface of 0.5-Cr/SiO<sub>2</sub>-MVS catalyst was comparable with the amount of active centers on the surface of SiO<sub>2</sub>-WI - the catalyst with ten times higher chromium loading.

#### 4. Conclusions

Presented data clearly indicate that metal vapour synthesis can be successfully applied to obtain Cr/SiO<sub>2</sub> catalytic materials, high active and selective in the reaction of propane oxidative dehydrogenation in the presence of CO<sub>2</sub>. The selectivity to main product – propylene was higher than 80% and as a main by-product it was produced another olefin – ethylene. Consequently, the

yield of propylene was ca. 40% and higher for all studied catalysts with the chromium loading higher than 0.5 wt%. Such a result superior the major part of the publicized data [15] and can be of the industrial interest. The use of metal vapor synthesis (MVS) technique allows to optimize the system in terms of activity (per Cr atom) and to obtain chromium species highly dispersed on the silica surface up to the high (6.0 wt%) chromium loadings. The catalytic activity should be related to the presence of chromate species of various nuclearity grafted on the silica surface. Chromium loading higher than 6.0 wt% did not result in the further increase of mono- or polychromate species but in the appearance on the catalyst surface of the  $\alpha$ -Cr<sub>2</sub>O<sub>3</sub> particles, not active in the investigated process. The formation of surface chromate species was also accompanied by the appearance of Brønsted acid sites, responsible for coke production, and relatively more abundant for higher Cr contents.

#### Acknowledgments

M.B. is recipient of a post-doc grant form Università di Torino - Regione Piemonte (Assegno C). The Compagnia di San Paolo (NIS sponsor) is acknowledged for financial support. Dr. Paolo Pertici is acknowledged for useful discussion.

## References

1. A.B. Gaspar, R.L. Martins, M. Schmal, L.C. Dieguez. *J. Mol. Catal. A: Chem.* 169 (2001) 105.
2. A.B. Gaspar, L.C. Dieguez. *Appl. Catal., A* 227 (2002) 241.
3. B.P. Liu, K. Fukuda, H. Nakatani, C. Nishiyama, M. Yamahiro, M. Terano. *J. Mol. Catal. A: Chem.* 219 (2004) 165.
4. A.B. Gaspar, C.A.C. Perez, L.C. Dieguez. *Appl. Surf. Sci.* 252 (2005) 939.
5. M.A. Botavina, G. Martra, Yu.A. Agafonov, N.A. Gaidai, N.V. Nekrasov, D.V. Trushin, S. Coluccia, A.L. Lapidus, *Appl. Catal. A* 347 (2008) 126.
6. S. Wang, K. Murata, T. Hayakawa, S. Hamakawa, R. Suzuki, *Appl. Catal. A* 196 (2000) 1.
7. S. Wang, K. Murata, T. Hayakawa, S. Hamakawa, R. Suzuki, *Catal. Lett.* 73 (2001) 107.
8. H. Yang, S. Liu, L. Xu, S. Xie, Q. Wang, L. Lin, *Stud. Surf. Sci. Catal.* 147 (2004) 697.
9. Y. Wang, Y. Ohishi, T. Shishido, Q. Zhang, W. Yang, Q. Guo, H. Wan, K. Takehira, *J. Catal.* 220 (2003) 347.
10. K. Takehira, Y. Ohishi, T. Shishido, T. Kawabata, K. Takaki, Q. Zhang, Y. Wang *J. Catal.* 224 (2004) 404.
11. J. Santamaria-Ganyales, J. Merida-Robles, M. Alcantara-Rodriguez, P. Maireles-Torres, E. Rodriguez-Castellon, A. Jimenez-Lopez, *Catal. Lett.* 64 (2000) 209.
12. I. Takahara, M. Saito, *Chem. Lett.*, 25 (1996) 973.
13. Y. Ohishi, T. Kawabata, T. Shishido, T. Ken, Zh. Qinghong, Y. Wang, *J. Mol. Catal. A*, 230 (2005) 49-58.
14. N. Mimura, M. Okamoto, H. Yamashita, S. Ted Oyama, K. Murata, *J. Phys. Chem. B*, 110 (2006) 21764-21770.
15. F. Cavani, N. Ballarini, A. Cericola, *Catal. Today* 127 (2007) 113.
16. M. Lezanska, G.S. Szymanski, P. Pietrzyk, Z. Sojka, J.A. Lercher, *J. Phys. Chem. C* 111 (2007) 1830.



17. M.S. Kumar, N. Hammer, M. Rønning, A. Holmen, D. Chen, J.C. Walmsleyb, G. Øye, J.Catal. 261 (2009) 116.
18. L. Zhang, Y. Zhao, H. Dai, H. He, C.T. Au, Catal Today 131 (2008) 42
19. K.J. Klabunde, Free Atoms, Clusters and Nanoscale Particles, Academic Press, New York, 1994.
20. J. S. Bradley in Cluster and Colloids: From Theory to Applications, Schmid (Ed.), VCH, Weinheim, 1994.
21. G. Vitulli, C. Evangelisti, A.M. Caporusso, P. Pertici, N. Panziera, S. Bertozzi, P. Salvadori in: B. Corain, G. Schmid, N. Toshima (Eds.), "Metal nanoclusters in catalysis and materials science: the issue of size-control", Elsevier, Amsterdam, 2008, chapter 32.
22. W.M. Lamanna, J. Am. Chem. Soc. 108 (1986) 2096.
23. L.A. Aronica, E. Schiavi, C. Evangelisti, A.M. Caporusso, P. Salvadori, G. Vitulli, L. Bertinetti, G. Martra, J. Catal. 266(2) (2009) 250.
24. G. Vitulli, C. Evangelisti, P. Pertici, A.M. Caporusso, N. Panziera, P. Salvadori, M.G. Faga, C. Manfredotti, G. Martra, S. Coluccia, A. Balerna, S. Colonna, S. Mobilio, J. Organomet. Chem. 681 (2003) 37.
25. C. Evangelisti, N. Panziera, P. Pertici, , G. Vitulli, P. Salvadori, C. Battocchio, G. Polzonetti, J. Catal., 262, 287-293 (2009).
26. E. Pitzalis, C. Evangelisti, N. Panziera, A. Basile, G. Capannelli, G. Vitulli in "Membrane for Membrane Reactors"; Elsevier (Amsterdam) (2010), *in press*.
27. a) B.M. Weckhuysen, L.M. De Ridder, R.A. Schoonheydt, J. Phys. Chem., 97 (1993) 4756; b) B.M. Weckhuysen, A.A. Verberckmoes, A.L. Buttiens, R.A. Schoonheydt, J. Phys. Chem., 98 (1994) 579; c) J.-M. Jehng, I.E. Wachs, B.M. Weckhuysen, R.A. Schoonheydt, J. Chem. Soc., Faraday Trans., 91 (1995) 953.
28. E. Groppo, C. Lamberti, S. Bordiga, G. Spoto, A. Zecchina, Chem. Rev. 105 (2005) 115.

29. G. Bellusi, G. Centi, S. Perathoner, F. Trifiro, in "Catalytic Selective Oxidation," p. 281. Am. Chem. Soc. Washington, DC, 1993.
30. A.A. Davydov, C.H. Rochester (Ed.), *Infrared Spectroscopy of Adsorbed Species on the Surface of Transition Metal Oxides*, Wiley, Chichester, 1990, p.27.
31. G. Busca, *Catal. Today* 41 (1998) 191.
32. Y. Hu, Sh. Higashimoto, G. Martra, J. Zhang, M. Matsuoka, S. Coluccia, M. Anpo, *Catal. Lett.* 90 (2003) 161.
33. K. Vikulov, G. Martra, S. Coluccia, D. Miceli, F. Arena, A. Parmaliana, E. Paukshtis, *Catal. Lett.* 37 (1996) 235.
34. G. Martra, F. Arena, S. Coluccia, F. Frusteri, A. Parmaliana, *Catal. Today* 63 (2000) 197.
35. G. Busca, L. Marchetti, G. Centi, F. Trifiro, *J. Chem. Soc., Faraday Trans. 1.* 81 (1985) 1003.
36. H. Miyata, K. Fuji, T. Ono, *J. Chem. Soc., Faraday Trans. 1.* 84 (1988) 3121.
37. B.A. Morrow, I.A. Cody, *J. Phys. Chem.* 79 (1975) 761.
38. B.A. Morrow, I.A. Cody, *J. Phys. Chem.* 80 (1976) 1995.
39. B.A. Morrow, I.A. Cody, *J. Phys. Chem.* 80 (1976) 1998

Table 1: Codes, composition and textural properties of the Cr/SiO<sub>2</sub> catalysts prepared by MVS (part A) and WI (part B, from [5]) technique

Part A					
Catalyst	Cr loading, wt%	specific surface area, m <sup>2</sup> /g	at.Cr/nm <sup>2</sup>	total pore volume, cm <sup>3</sup> /g	pore diameter, nm
bare silica (KSKG)	-	346	-	0.93	10.8
0.25-Cr/SiO <sub>2</sub> -MVS	0.25	318	0.09	0.89	11.2
0.5-Cr/SiO <sub>2</sub> -MVS	0.5	315	0.18	0.89	11.2
1.3-Cr/SiO <sub>2</sub> -MVS	1.3	306	0.49	0.86	11.2
2.5-Cr/SiO <sub>2</sub> -MVS	2.5	302	0.96	0.84	11.1
6.0-Cr/SiO <sub>2</sub> -MVS	6.0	300	2.32	0.78	10.3
10.0-Cr/SiO <sub>2</sub> -MVS	10.0	253	4.58	0.69	6.4
Part B*					
Catalyst	Cr loading, wt%	specific surface area, m <sup>2</sup> /g	at.Cr/nm <sup>2</sup>	total pore volume, cm <sup>3</sup> /g	pore diameter, nm
bare silica (KSKG)	-	346	-	0.93	10.8
0.5-Cr/SiO <sub>2</sub> -WI	0.5	315	0.18	0.86	10.9
1.0-Cr/SiO <sub>2</sub> -WI	1.0	314	0.37	0.86	10.9
3.0-Cr/SiO <sub>2</sub> -WI	3.0	310	1.12	0.84	10.9
5.0-Cr/SiO <sub>2</sub> -WI	5.0	307	1.89	0.82	10.7
7.5-Cr/SiO <sub>2</sub> -WI	7.5	272	3.19	0.77	10.8

\* - data taken from [5].

Table 2: Initial propane conversion (x), selectivity toward olefins (S) and yield of olefins (Y) obtained by using the Cr/SiO<sub>2</sub> catalysts prepared by MVS technique for ODH of propane in presence of CO<sub>2</sub>, T=600°C, w=200h-1, C<sub>3</sub>H<sub>8</sub>:CO<sub>2</sub>:N<sub>2</sub>=15:30:55

Cr, %	$x_{C_3H_8}$ , %	$S_{C_3H_6}$ , %	$S_{C_2H_4}$ , %	$S_{(C_3H_6+C_2H_4)}$ , %	$Y_{C_3H_6}$ , %	$Y_{(C_3H_6+C_2H_4)}$ , %
0.25	30.2	87.2	7.4	94.6	26	28
0.5	43.9	85.1	7.4	92.5	37	41
1.3	47.3	83.2	7.8	90.1	39	43
6.0	85.1	80.8	7.6	88.4	69	75
10.0	80.6	77.6	7.5	85.1	63	68

## Figure captions

Figure 1. TEM/EDS data obtained for the 0.5-Cr/SiO<sub>2</sub>-MVS sample: image (section A) and corresponding EDS map of the Cr (section B) and Si location (section C). Original magnification: 15k × (section A) and 8k × (section B).

Figure 2. TEM images of 10.0-Cr/SiO<sub>2</sub>-MVS, representative of the size and morphology of the  $\alpha$ -Cr<sub>2</sub>O<sub>3</sub> (section A) and silica (section B) phases. Original magnification: 30k ×.

Figure 3. DR UV-Vis spectra of the catalysts calcined in flowing O<sub>2</sub> at 600°C. Panel A: 1) 0.25-Cr/SiO<sub>2</sub>-MVS, 2) 0.5-Cr/SiO<sub>2</sub>-MVS, 3) 1.3-Cr/SiO<sub>2</sub>-MVS, 4) 2.5-Cr/SiO<sub>2</sub>-MVS, 5) 6.0-Cr/SiO<sub>2</sub>-MVS, 6) 10.0-Cr/SiO<sub>2</sub>-MVS. Panel B: 1) SiO<sub>2</sub>, 2) 0.5-Cr/SiO<sub>2</sub>-WI, 3) 1.0-Cr/SiO<sub>2</sub>-WI, 4) 3.0-Cr/SiO<sub>2</sub>-WI, 5) 5.0-Cr/SiO<sub>2</sub>-WI, 6) 7.5-Cr/SiO<sub>2</sub>-WI. Inset: spectrum of  $\alpha$ -Cr<sub>2</sub>O<sub>3</sub> treated in the same way.

Figure 4. IR spectra of NH<sub>3</sub> irreversible adsorbed at 298 K on ox/deg catalysts. Panel A: 1) SiO<sub>2</sub>, 2) 0.5-Cr/SiO<sub>2</sub>-MVS, 3) 1.3-Cr/SiO<sub>2</sub>-MVS, 4) 2.5-Cr/SiO<sub>2</sub>-MVS, 5) 6.0-Cr/SiO<sub>2</sub>-MVS, 6) 10.0-Cr/SiO<sub>2</sub>-MVS. Panel B: 1) SiO<sub>2</sub>, 2) 0.5-Cr/SiO<sub>2</sub>-WI, 3) 1.0-Cr/SiO<sub>2</sub>-WI, 4) 3.0-Cr/SiO<sub>2</sub>-WI, 5) 5.0-Cr/SiO<sub>2</sub>-WI, 6) 7.5-Cr/SiO<sub>2</sub>-WI.

Figure 5. Catalytic properties vs. reaction time in the reaction of ODH of propane, T=600°C, w=200h<sup>-1</sup>, reaction mixture C<sub>3</sub>H<sub>8</sub>:CO<sub>2</sub>:N<sub>2</sub>=15:30:55 on the: 1- 0.5-Cr/SiO<sub>2</sub>-MVS; 2 - 5.0-Cr/SiO<sub>2</sub>-WI catalysts. Panel A: C<sub>3</sub>H<sub>8</sub> conversion. Panel B: Total selectivity to olefins (curves a) and total olefin yield (curves b).

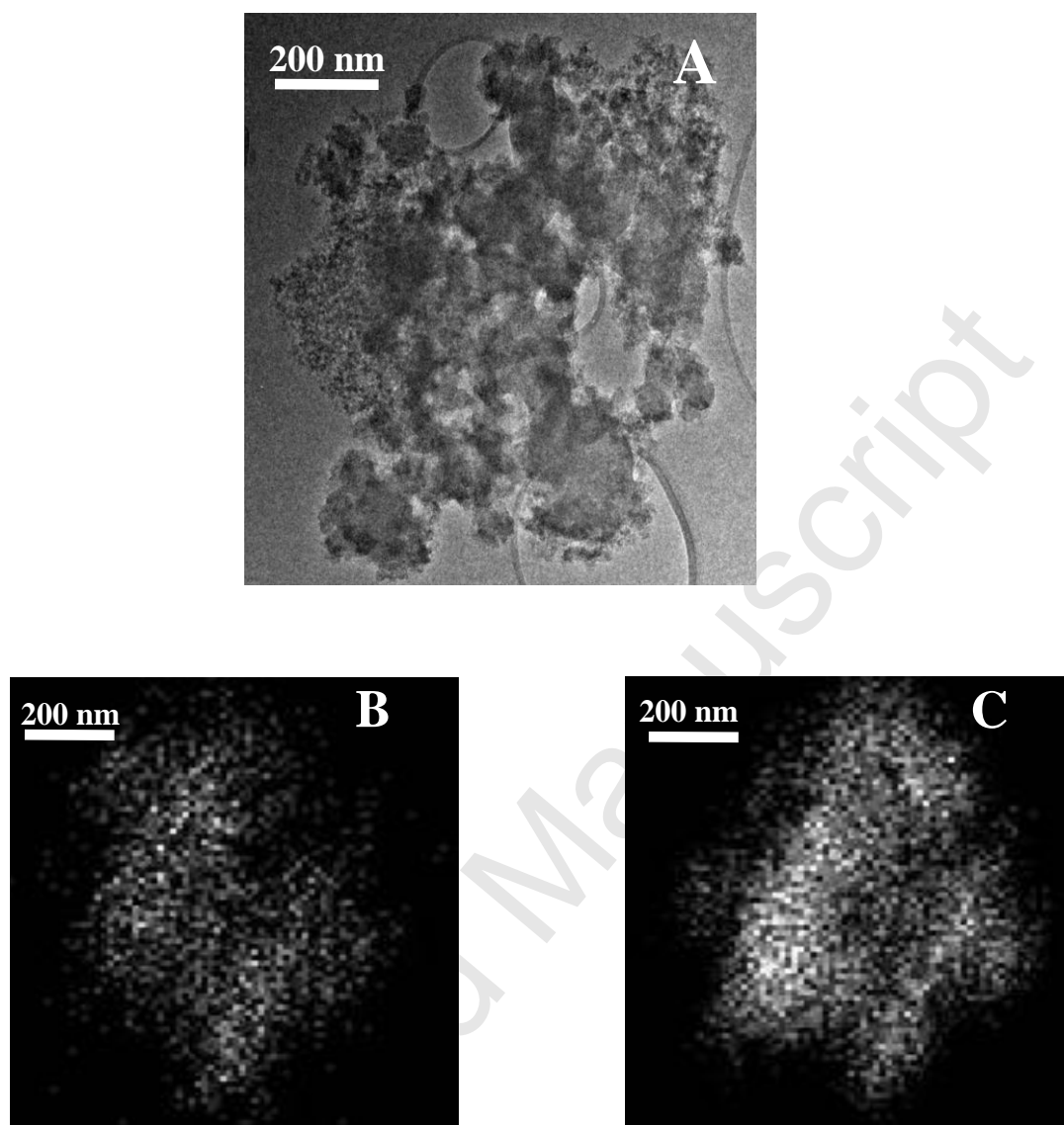


Figure 1

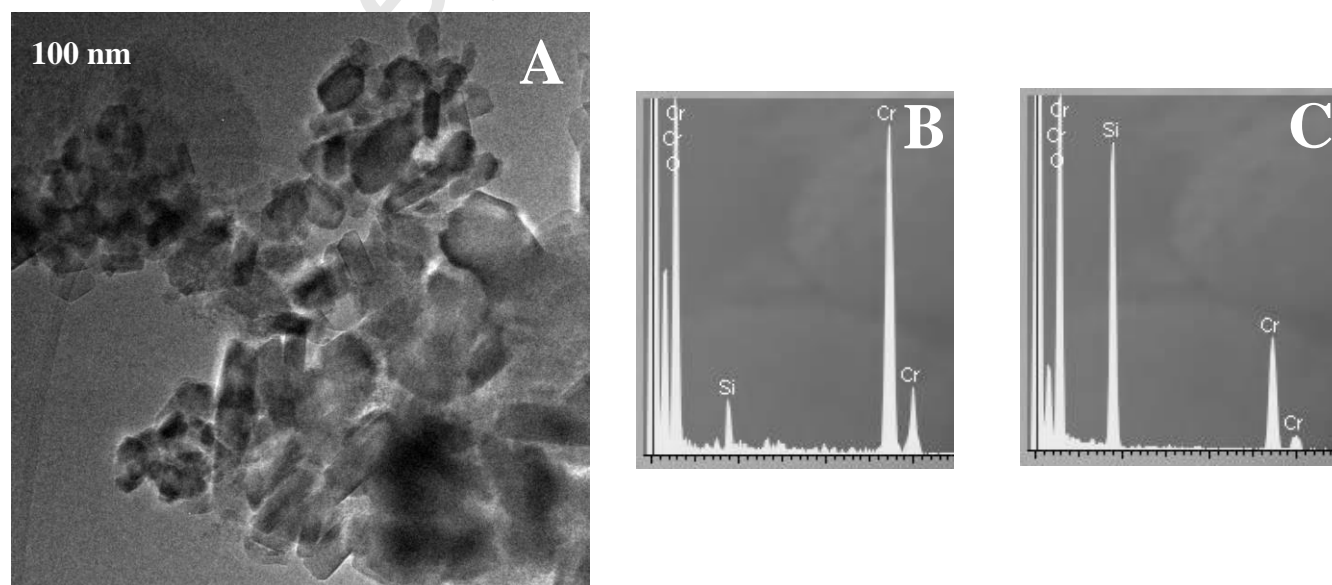


Figure 2

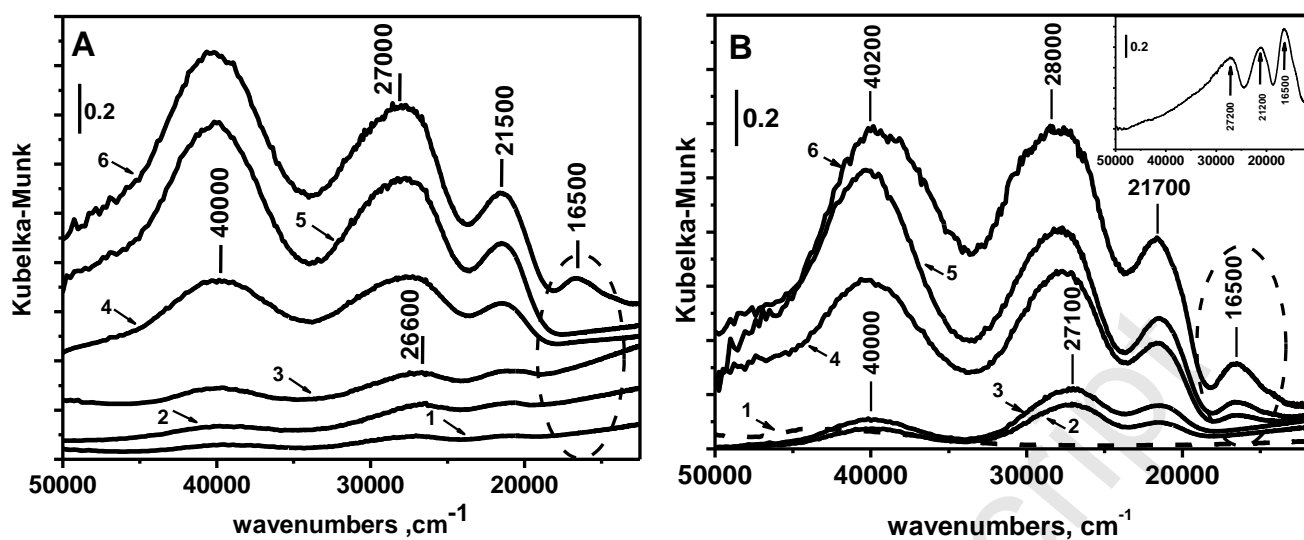


Figure 3

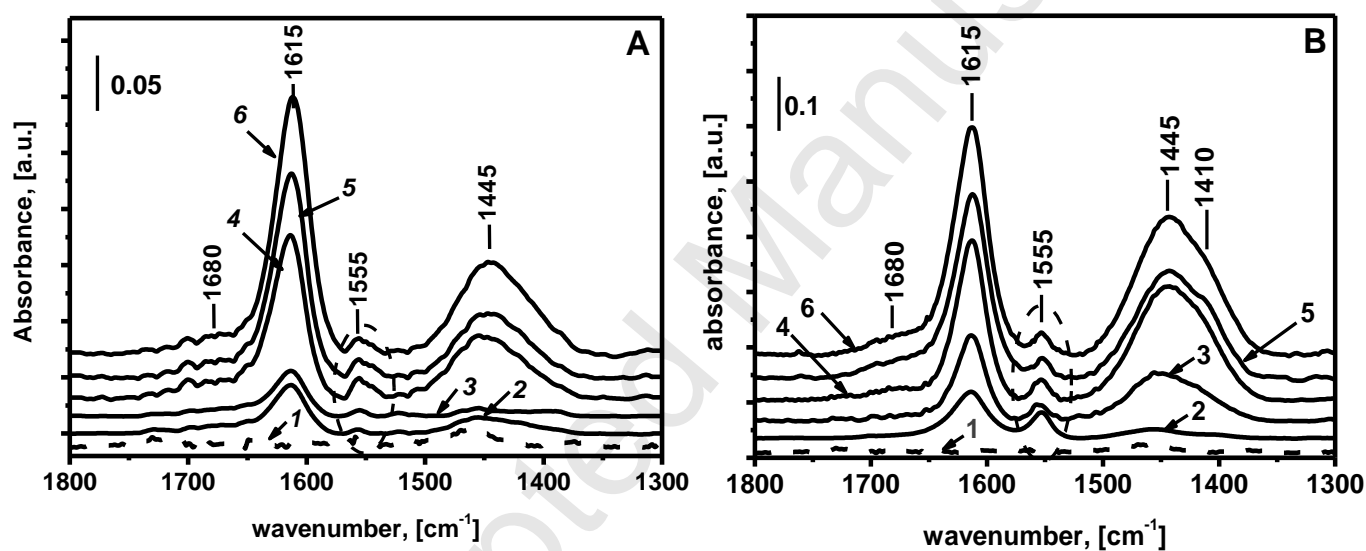


Figure 4

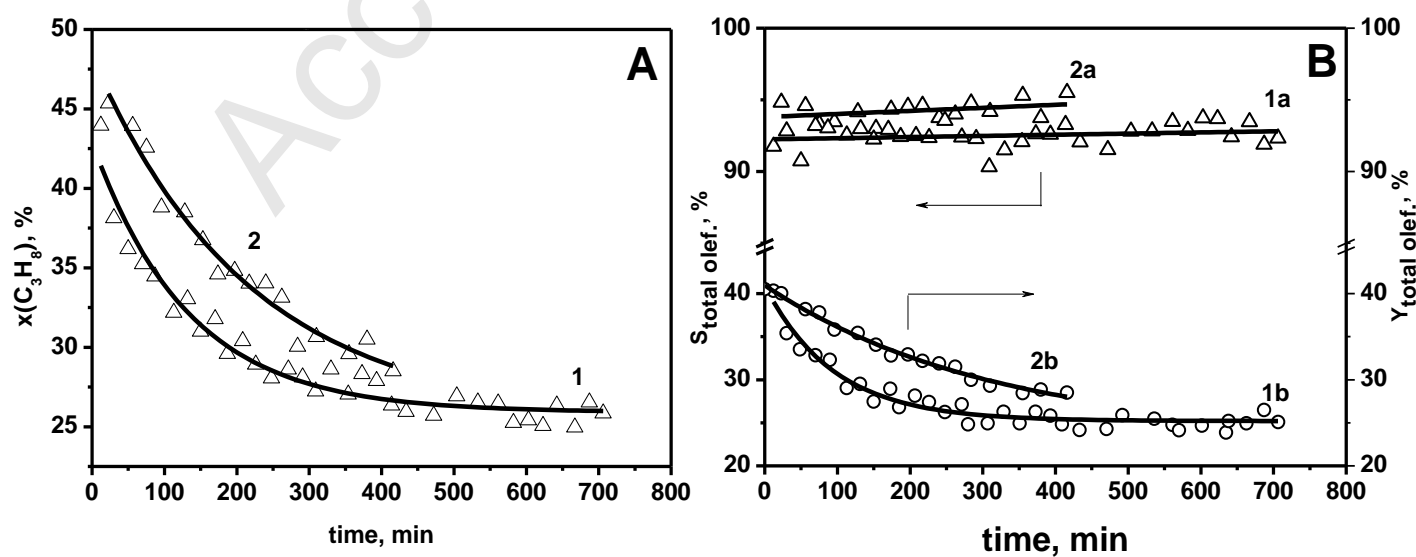


Figure 5